Analytic Born completion in the calculation of differential cross sections for electron scattering from a linear molecule

Andrew N. Feldt* and Michael A. Morrison†

Homer L. Dodge Department of Physics and Astronomy, University of Oklahoma, Norman, Oklahoma 73019-2061, USA

(Received 31 January 2007; revised manuscript received 29 November 2007; published 31 January 2008)

We present a closed-form expression for the infinity of high-order partial waves and symmetry classes required to converge differential cross sections for vibrationally elastic or inelastic electron scattering from a linear molecule. This expression combines correction terms based on the first Born approximation with terms that contain T-matrix elements from accurate, non-Born scattering calculations such as those of body-frame fixed-nuclear-orientation theory. The equations for analytic Born completion reduce the convergence requirements for a differential cross section from several potentially infinite sums over angular-momentum quantum numbers to a single parameter that determines the partial-wave order at which the switch to the Born approximation occurs. We demonstrate the efficacy and accuracy of these equations for low-energy collisions of electrons with H_2 and N_2.

DOI: 10.1103/PhysRevA.77.012726 PACS number(s): 34.80.Bm, 34.80.Gs

I. INTRODUCTION

Calculation of a differential cross section (DCS) usually begins with calculation of theoretical scattering quantities—phase shifts for scattering from a central potential, scattering matrices for a nonspherical interaction, and/or scattering from a target with internal structure. Computing such quantities often takes so much effort that difficulties involved in the final step—using the computed quantities to evaluate the cross section—may be marginalized. Yet, this final step presents its own numerical and practical difficulties, especially for electron-molecule scattering, where internal target structure is always important, the interaction is never spherically symmetric and, strictly speaking, there are no phase shifts. Foremost among these difficulties are matters of convergence, the concerns of this paper.

Expressions for electron-molecule DCS contain complicated interference among elements of the transition (T) matrix [see Eqs. (6a)–(6c) below]. For a closed-shell, linear target, for example, one must converge seven infinite sums [1,2]: four over values of the quantum number l for the scattering electron's orbital angular momentum, two over the quantum number Λ for the projection of $\hat{l}$ along the axis of spatial quantization, and one in the Legendre expansion of the DCS. Because most molecules are highly aspherical, and because the slowly decaying electron-molecule interaction typically influences the scattering function even at very large distances from the target, the number of terms required to converge each of these sums may be huge. This problem is especially acute at the low scattering energies.

This potentially serious situation is greatly ameliorated by the applicability of the first Born approximation (FBA) for scattering quantities of high partial-wave order [3–11]. The accuracy of the FBA, which increases with partial-wave order l, derives from terms in the radial scattering equations that result from the electron's angular kinetic-energy operator. These centrifugal-barrier terms effectively "exclude" high-order components of the scattering function from the strong-potential region near the target. These components are therefore determined entirely by the region far from the target, where the potential is comparatively weak. For sufficiently high partial-wave orders, elements of the scattering matrix can be accurately approximated by a weak-scattering theory such as the FBA (see Ref. [9] and citations therein). The accuracy of the FBA for a given partial-wave component actually improves as the electron's incident energy decreases toward threshold: the smaller the energy, the lower the order of partial wave at which the FBA attains a given degree of accuracy.

This underlying physics justifies the idea of "Born completion" [6,8,9,11], which some authors call "Born closure" [6–8]. One chooses a partial-wave order l_B and, for all $l > l_B$, calculates contributions to the DCS [4,6,9,11] (or scattering amplitude [3,7,8]) in the FBA, using as the potential the simple, closed-form asymptotic ("long-range") multipole expansion [see Eq. (8a) below]. In principle, this gambit allows completion to infinity of all angular momentum sums without the need to calculate scattering-matrix elements by more demanding means such as solution of close-coupling equations.

In both electron-atom and -molecule scattering, Born completion is often implemented via a purely numerical procedure (see, for example, Refs. [12–17]). At each scattering energy, one includes more and more FBA terms—that is, terms which, for $l > l_B$, are calculated using the FBA—until the DCS converges to the desired precision at all angles. This procedure, which we shall call numerical Born completion (NBC), requires careful, sometimes extensive convergence studies, as truncating infinite sums over partial-wave order at too small a value can induce artificial, unphysical oscillations in the DCS, especially at scattering angles less than a few tens of degrees (see, for example, Sec. III of Ref. [14]). In Sec. III we use NBC to illustrate the usefulness and accuracy of the alternative, analytic Born completion presented in this paper.

The equations of analytic Born completion (ABC), which are derived for vibrationally inelastic (and elastic [9]) scat-

*feldt@nhn.ou.edu

†www.nhn.ou.edu/~morrison; morrison@nhn.ou.edu

tering in Sec. II, simplify convergence and eliminate the need to calculate the many FBA T-matrix elements required for numerical Born completion. Here as in other applications of analytic Born completion, the objective is a closed-form expression one can add to a finite sum of non-Born, low-order contributions to complete to infinity all sums in the DCS [18].

The idea of using the first Born approximation to analytically complete a DCS predates the modern era of computational electron-molecule physics. In 1966, Thompson [3], noting the weak scattering of high-order partial waves in low-energy collisions, used the closed-form (analytic) expression for the FBA to complete the infinite the sum over partial-wave order in the scattering amplitude for elastic scattering from Ne and Ar. Thompson's idea was subsequently developed (see, for example, Refs. [19] and [20]) and remains in wide use in modern electron-atom calculations (see, for example, Ref. [21]).

In 1971, Crawford and Dalgarno [4] extended this idea to low-energy elastic scattering and rotational excitation from CO; in contrast to Thompson, Crawford and Dalgarno applied the analytic FBA directly to the lab-frame differential cross section, written as an infinite sum over Legendre polynomials. In 1982, Norcross and Padial [6] combined this use of the FBA with complete sums over partial-wave orders in the lab-frame rovibrational DCS using low-order T-matrix elements calculated in the adiabatic-nuclear-rotation approximation (Ref. [1], and references therein). The resulting "multipole-extracted adiabatic-nuclei approximation" was subsequently extended and applied by Norcross and collaborators to several systems (for a review and citations, see Sec. V.A.1 of Ref. [22]).

At about the same time, this idea was extended to electronic excitation. In 1980, Fliflet and Mckoy [5] treated electronic excitation of H_2, using the FBA and expansions of the target electronic orbitals in Cartesian Gaussian functions (see Ref. [5], Appendix) to develop closed-form (analytic) approximations to the high-order fixed-nuclei dynamical coefficients that appear in the scattering amplitude in the angular-momentum-transfer formulation [23]. In a 1992 application of the complex Kohn variational method [24] to the ($\pi \rightarrow \pi^*$) excitation of ethylene, Rescigno and Schneider (Ref. [7], Sec. III) numerically constructed lab-frame cross sections from partial-wave T-matrix elements by applying Born closure idea to the scattering amplitudes.

That same year, in complex-Kohn calculations of low-energy electronically elastic scattering from NH_3, Rescigno *et al.* [8] used a similar hybrid treatment to rectify the notorious divergence at all angles of the partial-wave expansion of body-fixed T matrix from adiabatic-nuclei calculations. These authors emphasized the advantages for polar targets of applying their closure formula to the scattering amplitude.

Building on these conceptual and formal foundations, Isaacs and Morrison [9,10] developed and implemented the present analytic Born completion (ABC) procedure. Their development was, however, restricted to vibrationally elastic scattering. Subsequently, this development was elaborated and used by others (see, for example, Refs. [25–33]). In 2000, Itikawa [11] derived an analytic completion technique for polar molecules [11], as we discuss in the context of Sec. II.

The present paper derives (Sec. II), a generalization of the work of Isaacs and Morrison that removes the restriction to vibrationally elastic scattering. These equations apply not only to diatomic targets but also to such polyatomic targets as CO_2 and acetylene provided the excitation of interest is in a "nonpolar" mode (e.g., symmetric stretch excitations of CO_2), and the cross sections of interest is not influenced by coupling to "polar" modes (asymmetric stretch and bending) [34]. To explore the utility and accuracy of this analytic procedure and to compare it to numerical Born completion, we present in Sec. III applications to two paradigmatic homonuclear diatomic systems e-H_2 and e-N_2. Unless otherwise indicated, we use atomic units throughout.

II. THEORY

A. Context

The theoretical context for this work is the body-frame (BF) formulation of electron-molecule scattering in the fixed-nuclear-orientation (FNO) approximation [35–37]. In BF-FNO theory, *vibrational* dynamics are not treated adiabatically; this theory is therefore not beset by the sometimes appreciable error that can appear in adiabatic-nuclear-vibration cross sections [38,39]. Furthermore, the BF-FNO formulation ensures proper inclusion of nonadiabatic effects, which here involve energy transfer between the kinetic energy of the electron and the vibrational energy of the molecule. We thus calculate low-order non-Born T-matrix elements using the now-standard BF vibrational close-coupling method (also called the "hybrid theory" [40,41]). Details and further citations appear in reviews by one of the present authors: for the underlying physics, see Ref. [42]; for the formal theory, Ref. [22]; and for practical implementation, Ref. [2].

B. Differential cross sections for electron-molecule scattering

If the scattering energy is large compared to the molecule's rotational constant, then the treatment of inelastic scattering can be simplified via the aforementioned FNO approximation without significant attendant error [1,14,22]. The scattering amplitude $f(\boldsymbol{k}_v,\boldsymbol{k}_0;\hat{\boldsymbol{R}})$ then depends on $\hat{\boldsymbol{R}}$ only parametrically. The measured differential cross section (DCS) is obtained via an average over angles

$$\frac{d\sigma}{d\Omega}(\boldsymbol{k}_v,\boldsymbol{k}_0) = \frac{1}{4\pi}\frac{k_v}{k_0}\int |f(\boldsymbol{k}_v,\boldsymbol{k}_0;\hat{\boldsymbol{R}})|^2 d\hat{\boldsymbol{R}}, \tag{1}$$

where $\boldsymbol{k}_0$ and $\boldsymbol{k}_v$ are the initial and final wave vectors for the scattering electron. We define the scattering amplitude as [43]

$$f(\boldsymbol{k}_v,\boldsymbol{k}_0;\hat{\boldsymbol{R}}) \equiv -\frac{m_e}{2\pi\hbar^2}\langle v,\boldsymbol{k}_v|\hat{T}(E+i0)|v_0,\boldsymbol{k}_0\rangle, \tag{2}$$

using v_0 and v for the vibrational quantum numbers in the entrance and exit channels, respectively. Here, $\hat{T}(E+i0)$ is the on-shell T operator (Refs. [44] and [45], Sec. III) for total energy

$$E = \frac{\hbar^2 k_v^2}{2m_e} + \epsilon_v \tag{3}$$

for a channel with the molecule in a (Born-Oppenheimer) vibrational state of energy ϵ_v and the electron with wave number k_v. We denote quantities that signify the entrance channel (initial vibrational quantum number v_0) by the single subscript 0, as $\boldsymbol{k}_0$ rather than $\boldsymbol{k}_{v_0}$.

In single-center formulations [46], the scattering amplitude is transformed from momentum space to a basis of angular-momentum eigenstates as (see Sec. 2 of Ref. [22])

$$f(\boldsymbol{k}_v,\boldsymbol{k}_0;\hat{\boldsymbol{R}}) = \sum_{l,l_0}\sum_{m,m_0} \langle \boldsymbol{k}_v|E_v lm\rangle f_{vlm,v_0 l_0 m_0}(k_v,k_0;\hat{\boldsymbol{R}}) \times \langle E_0 l_0 m_0|\boldsymbol{k}_0\rangle, \tag{4}$$

where $E_v \equiv \hbar^2 k_v^2/2m_e$, and the expansion coefficients of a plane-wave-normalized free-particle plane-wave state $|\boldsymbol{k}_v\rangle$ in the energy-normalized basis $\{|E_v lm\rangle\}$ are (Ref. [45], Sec. VII.B)

$$\langle E_v lm|\boldsymbol{k}_v\rangle = i^l \left(\frac{\hbar^2}{m_e}\right)^{1/2} k_v^{-1/2} Y_{l,m}^*(\hat{\boldsymbol{k}}). \tag{5}$$

(Throughout this paper, formal sums over orbital angular momentum quantum numbers l run from 0 to ∞ and sums over m and Λ run from $-l$ to $+l$.) In Eq. (4) the quantum numbers (l,m) refer to the orbital angular momentum of the scattering electron, where m corresponds to the space-fixed ("lab frame") z axis. The partial-wave scattering amplitudes $f_{vlm,v_0 l_0 m_0}(k_v,k_0;\hat{\boldsymbol{R}})$ defined by Eq. (4) are thus inherently lab-frame quantities and must be related to the body-frame T-matrix elements via Euler angle rotations [2].

These rotations, followed by a good deal of algebra, result in an equation for the DCS of Eq. (1) as a sum over Legendre polynomials of the lab-frame scattering angle $\theta \equiv \hat{\boldsymbol{r}}\cdot\hat{\boldsymbol{R}}$ (see Ref. [1], and references therein):

$$\frac{d\sigma}{d\Omega}(\boldsymbol{k}_v,\boldsymbol{k}_0) = \frac{\pi^2}{k_0}\sum_{L=0}^{\infty} B_L(v_0 \to v) P_L(\cos\,\theta). \tag{6a}$$

The BF-FNO T-matrix elements $T^{\Lambda}_{vl,v_0 l_0}$ appear in the expansion coefficients

$$B_L(v_0 \to v) \equiv \sum_{l,l_0}\sum_{l',l_0'}\sum_{\Lambda,\Lambda'} d_L(ll_0,l'l_0';\Lambda,\Lambda') T^{\Lambda *}_{vl,v_0 l_0} T^{\Lambda'}_{vl',v_0 l_0'}. \tag{6b}$$

This definition collapses the effects of the transformation to an angular-momentum basis [Eq. (5)], followed by rotation into the BF, into the coefficients

$$d_L(ll_0,l'l_0';\Lambda,\Lambda') \equiv i^{l_0'-l'-l_0+l}[(2l+1)(2l_0+1)(2l'+1)(2l_0'+1)]^{1/2} \times (2L+1)\begin{pmatrix} l & l' & L \\ 0 & 0 & 0 \end{pmatrix}\begin{pmatrix} l_0 & l_0' & L \\ 0 & 0 & 0 \end{pmatrix}\begin{pmatrix} l & l' & L \\ \Lambda & -\Lambda' & \Lambda'-\Lambda \end{pmatrix}\begin{pmatrix} l_0 & l_0' & L \\ \Lambda & -\Lambda' & \Lambda'-\Lambda \end{pmatrix}. \tag{6c}$$

For Wigner $3j$ symbols we use the notation of Ref. [47]; for notation and conventions of other authors and for relations required to derive Eq. (6c), see Chap. 8 of Varshalovich *et al.* [48]. The quantum number Λ corresponds to the projection of the electron's orbital angular momentum along the internuclear axis, the z axis of the BF frame [49]. For given l and l_0, the sums over Λ run from $-\bar{l}$ to $+\bar{l}$, where $\bar{l} \equiv \min(l,l_0)$.

C. The Born approximation in low-energy electron-molecule scattering

The first Born approximation (FBA) to the exact scattering amplitude $f(\boldsymbol{k}_v,\boldsymbol{k}_0;\hat{\boldsymbol{R}})$, as used in the derivation of Sec. II D, follows from the definition (2). One first relates the on-shell T operator to the interaction potential energy V, then neglects scattering effects in the entrance channel by replacing the plane-wave scattering state in this channel by a free wave to obtain (Ref. [45], Sec. IV.A)

$$f^B(\boldsymbol{k}_v,\boldsymbol{k}_0;\hat{\boldsymbol{R}}) = -4\pi^2\left(\frac{m_e}{\hbar^2}\right)\langle v,\boldsymbol{k}_v|V|v_0,\boldsymbol{k}_0\rangle, \tag{7a}$$

$$= -\frac{1}{2\pi}\int e^{i\boldsymbol{q}_{v,v_0}\cdot\boldsymbol{r}}\langle v|V|v_0\rangle d\boldsymbol{r}, \tag{7b}$$

where $\boldsymbol{q}_{v,v_0} \equiv \boldsymbol{k}_0 - \boldsymbol{k}_v$ is the momentum transfer vector, and the vibrational matrix element $\langle v|V|v_0\rangle$ implies integration over the internuclear separation R. Validity of the FBA for low-energy electron scattering is assured by using in Eqs. (7a) and (7b) the long-range (LR) multipole expansion of the potential. For a linear target the first three terms in this expansion are

$$V_{\mathrm{LR}}(\boldsymbol{r},R) = -\frac{\alpha_0(R)}{2r^4} - \frac{d(R)}{r^2}P_1(\cos\,\theta) - \left[\frac{Q(R)}{r^3} + \frac{\alpha_2(R)}{2r^4}\right]P_2(\cos\,\theta). \tag{8a}$$

The terms in Eq. (8a) include four properties of the target: its permanent dipole and quadrupole moments $d(R)$ and $Q(R)$, and its induced spherical and nonspherical polarizabilities $\alpha_0(R)$ and $\alpha_2(R)$ [50,51]. For some highly aspherical systems, such as e-CO_2, calculations of DCS require higher-

order terms (e.g., permanent octupole [52]). In the ABC results of Sec. II D, we allow for this possibility by using the generic multipole expansion

$$V_{\mathrm{LR}}(\boldsymbol{r},R)=\sum_{\lambda,\eta}\frac{b_{\lambda,\eta}(R)}{r^{\eta}}P_{\lambda}(\cos\,\theta). \tag{8b}$$

The sum over λ runs from $\lambda=0$ [the spherical-polarizability term in Eq. (8a)] to a finite upper limit chosen to include all necessary permanent and induced moments; for homonuclear molecules only even values of $\lambda\geq 0$ appear in this sum. The second index η controls the dependence of each term on r and allows for the inclusion in a particular Legendre projection in Eq. (8b) of both a permanent and an induced moment, as is necessary for $\lambda=2$ in Eq. (8a). In this notation the moments in Eq. (8a) are $b_{1,2}(R)=-d(R)$, $b_{2,3}(R)=-Q(R)$, $b_{0,4}(R)=-\alpha_0(R)/2$, and $b_{2,4}(R)=-\alpha_2(R)/2$.

When this long-range potential is used in vibrational close-coupling calculations, there result potential matrix elements in the coupled scattering equations that contain vibrational matrix elements $\langle v'|b_{\lambda,\eta}(R)|v\rangle$ for all coefficients $b_{\lambda,\eta}(R)$ one includes in Eq. (8b). Explicit expressions for these matrix elements and details regarding their calculation appear in Ref. [2] and in Sec. III.A of Ref. [17].

D. The equations of analytic Born completion

Following the strategy of previous work discussed in Sec. I, we now add to and subtract from the exact scattering amplitude $f(\boldsymbol{k}_v,\boldsymbol{k}_0;\hat{\boldsymbol{R}})$ its Born approximate, viz.,

$$\begin{aligned}f(\boldsymbol{k}_v,\boldsymbol{k}_0;\hat{\boldsymbol{R}})=&\sum_{l,l_0}\sum_{m,m_0}\langle\boldsymbol{k}_v|E_vlm\rangle f_{vlm,v_0l_0m_0}(k_v,k_0;\hat{\boldsymbol{R}})\\&\times\langle E_0l_0m_0|\boldsymbol{k}_0\rangle+[f^B(\boldsymbol{k}_v,\boldsymbol{k}_0;\hat{\boldsymbol{R}})\\&-\sum_{l,l_0}\sum_{m,m_0}\langle\boldsymbol{k}_v|E_vlm\rangle f^B_{vlm,v_0l_0m_0}(k_v,k_0;\hat{\boldsymbol{R}})\\&\times\langle E_0l_0m_0|\boldsymbol{k}_0\rangle],\end{aligned} \tag{9a}$$

where $f^B_{vlm,v_0l_0m_0}(k_v,k_0;\hat{\boldsymbol{R}})$ is a lab-frame partial-wave scattering amplitude in the Born approximation. If all sums in Eq. (9a) could be evaluated to their maximum upper limits, this equation would reduce to a trivial tautology: the quantity in braces would equal zero and the expression would collapse to the usual partial-wave expansion of Eq. (4). The goal of ABC is to perform the sums over l and l' only up to a finite upper limit l_B yet include all contributing partial waves in the DCS.

Deriving the ABC equations for the vibrationally inelastic DCS from Eq. (9a) requires a good deal of algebra, none of which we reproduce here. (A detailed derivation is available as a MATHEMATICA notebook from the authors.) Instead we briefly summarize key steps.

We first rewrite Eq. (9a) as

$$\begin{aligned}f(\boldsymbol{k}_v,\boldsymbol{k}_0;\hat{\boldsymbol{R}})=&f^B(\boldsymbol{k}_v,\boldsymbol{k}_0;\hat{\boldsymbol{R}})+\sum_{l,l_0}^{l_B}\sum_{m,m_0}\langle\boldsymbol{k}_v|E_vlm\rangle\\&\times[f_{vlm,v_0l_0m_0}(k_v,k_0;\hat{\boldsymbol{R}})-f^B_{vlm,v_0l_0m_0}(k_v,k_0;\hat{\boldsymbol{R}})]\\&\times\langle E_0l_0m_0|\boldsymbol{k}_0\rangle.\end{aligned} \tag{9b}$$

[In practice we choose the incident wave vector $\boldsymbol{k}_0$ to lie along the lab-frame z axis so that $m_0=0$, $\hat{\boldsymbol{k}}_0=(0,0)$, and all spherical harmonics of $\hat{\boldsymbol{k}}_0$ are constants.] The FBA scattering amplitude is given in terms of the momentum transfer by Eq. (7b). Note that the angles (θ_q,ϕ_q) associated with $\boldsymbol{q}_{v,v_0}$ can be related to the angles (θ_k,ϕ_k) associated with $\boldsymbol{k}_v$ via

$$\cos\,\theta_q=\frac{k_0-k_v\cos\,\theta_k}{q_v}, \tag{10a}$$

$$\phi_q=\phi_k+\pi, \tag{10b}$$

where for clarity we omit vibrational subscripts from all angles. The FBA partial-wave scattering amplitudes in Eq. (9b) are

$$\begin{aligned}f^B_{vlm,v_0l_0m_0}(k_v,k_0;\hat{\boldsymbol{R}})=&-8\pi\sqrt{k_vk_0}\int j_l(k_vr)Y^*_{lm}(\hat{\boldsymbol{r}})V^{\mathrm{LR}}_{v,v_0}(\boldsymbol{r};\hat{\boldsymbol{R}})\\&\times j_{l_0}(k_0r)Y_{l_0m_0}(\hat{\boldsymbol{r}})d\boldsymbol{r},\end{aligned} \tag{11}$$

where $j_l(k_vr)$ is the spherical Bessel function [44], and $V^{\mathrm{LR}}_{v,v_0}(\boldsymbol{r};\hat{\boldsymbol{R}})=\langle v|V_{\mathrm{LR}}|v_0\rangle$ is the vibrational matrix element of the long-range interaction potential (8b).

Two special cases are noteworthy. First, setting $l_B=-1$ in Eq. (9b) generates pure-Born cross sections, which assume weak scattering in all partial waves and incorporate only the long-range interactions of Eq. (8b). Second, setting l_B in Eq. (9b) to ∞ reduces the right-hand side to the standard result for the scattering amplitude in terms of partial waves (Ref. [1], Sec. II.E). In the ABC procedure, however, we choose a finite $l_B\geq 0$ so that for $l>l_B$ the differences $f_{vlm,v_0l_0m_0}(k_v,k_0;\hat{\boldsymbol{R}})-f^B_{vlm,v_0l_0m_0}(k_v,k_0;\hat{\boldsymbol{R}})$ are negligible to the desired precision. Contributions to $f(\boldsymbol{k}_v,\boldsymbol{k}_0;\hat{\boldsymbol{R}})$ for $l>l_B$ are thus included in the FBA; those for $l\leq l_B$ are generated in non-Born calculations—here, via BF vibrational close coupling—that take account of the strong short- and intermediate-range electron-molecule interactions.

Inserting the long-range potential Eq. (8b) into Eq. (7b), we obtain

$$f^B(\boldsymbol{k}_v,\boldsymbol{k}_0;\hat{\boldsymbol{R}})=-2\sum_{\lambda,\eta}i^{\lambda}\langle v|b_{\lambda,\eta}|v_0\rangle P_{\lambda}(\hat{\boldsymbol{q}}\cdot\hat{\boldsymbol{R}})I^{\eta}_{\lambda}(q_{v,v_0}). \tag{12a}$$

Here we have introduced the integral

$$I_\lambda^\eta(q_{v,v_0}) \equiv \int_0^\infty j_\lambda(q_{v,v_0}r)r^{2-\eta}dr, \tag{12b}$$

which is defined only for $\eta>1$ and $\lambda>\eta>3$. For these values, this integral equals the function

$$M_\lambda^\eta(q_{v,v_0}) \equiv \sqrt{\pi}2^{1-\eta}q_{v,v_0}^{\eta-3}\left[\frac{\Gamma\left(\frac{3+\lambda-\eta}{2}\right)}{\Gamma\left(\frac{\lambda+\eta}{2}\right)}\right], \tag{12c}$$

where the reason for a separate symbol for $M_\lambda^\eta(q_{v,v_0})$ will become apparent in discussion of Eq. (17) below. [The restrictions on λ and η affect the integral $I_\lambda^\eta(q_{v,v_0})$ that arises from the spherical term $\lambda=0$ in Eq. (8b), which for $\eta=4$ is undefined—a point we will discuss further in conjunction with Eqs. (16a) and (16b) below.]

Similarly, inserting the long-range potential (8b) into Eq. (11) gives

$$f^{\mathcal{B}}_{vlm,v_0l_0m_0}(k_v,k_0;\hat{\boldsymbol{R}}) = -16\pi^{3/2}\sqrt{k_vk_0}\sum_{\lambda,\eta}\langle v|b_{\lambda,\eta}|v_0\rangle\frac{\sqrt{l+1}}{2\lambda+1} \times c_\lambda(lm,l_0m_0)I_{ll_0}^\eta(k_vk_0)Y^*_{\lambda,m-m_0}(\hat{\boldsymbol{R}}). \tag{13a}$$

The integral

$$I_{ll_0}^\eta(k_vk_0) \equiv \int_0^\infty j_l(k_vr)j_{l_0}(k_0r)r^{2-\eta}dr, \tag{13b}$$

is defined provided $l_0+l-\eta+3>0$, and $\eta>0$. For these values, this integral equals the function

$$M_{ll_0}^\eta(k_vk_0) \equiv \left(\frac{\pi}{2^\eta}\right)\frac{k_v^l}{k_0^{l-\eta+3}}\left[\frac{\Gamma\left(\frac{l_0+l-\eta+3}{2}\right)}{\Gamma\left(\frac{l_0-l+\eta}{2}\right)\Gamma\left(l+\frac{3}{2}\right)}\right] \times {}_2F_1\left(\frac{l_0+l-\eta+3}{2},\frac{l-l_0-\eta+2}{2},l+\frac{3}{2};\frac{k_v^2}{k_0^2}\right), \tag{13c}$$

where ${}_2F_1(a,b,c;z)$ is the hypergeometric function in the notation of Ref. [53]. Finally, the angular-momentum coefficient in Eq. (13a) is

$$c_\lambda(lm,l_0m_0) \equiv (-1)^{m-m_0}\sqrt{(2l_0+1)(2\lambda+1)} \times \begin{pmatrix} l & l_0 & \lambda \\ m & 0 & -m \end{pmatrix}\begin{pmatrix} l & l_0 & \lambda \\ m_0 & -m_0 & 0 \end{pmatrix}. \tag{14}$$

The partial-wave scattering amplitude can be written in terms of BF-FNO T-matrix elements as

$$f_{vlm,v_0l_0m_0}(k_v,k_0;\hat{\boldsymbol{R}}) = -4\pi^2\sum_\Lambda \mathcal{D}^l_{m,\Lambda}(\hat{\boldsymbol{R}})T^\Lambda_{vl,v_0l_0}\mathcal{D}^{l_0*}_{m_0,\Lambda}(\hat{\boldsymbol{R}}), \tag{15}$$

where $\mathcal{D}^l_{m,\Lambda}(\hat{\boldsymbol{R}})$ are Wigner rotation matrices in the conventions of Ref. [54]. Inserting Eqs. (12a), (13a), and (15) into Eq. (9b), using the result in Eq. (1), and carrying out various tiresome algebraic simplifications, we obtain the final ABC expression, here written in a form that facilitates encoding:

$$\frac{d\sigma}{d\Omega}(\boldsymbol{k}_v,\boldsymbol{k}_0) = \frac{1}{4\pi}\left(\frac{k_v}{k_0}\right)\sum_\lambda\sum_{m=-\lambda}^{\lambda} g^*_{\lambda,m}(\theta)g_{\lambda,m}(\theta) + 2\pi\sqrt{\frac{k_v}{k_0^3}}\sum_{l,l_0}^{l_B}\sum_{\Lambda,\lambda}\sum_{m=-\lambda}^{\lambda} c_\lambda(l_m,l_0\Lambda)Y_{l,m}(\hat{\boldsymbol{k}}) \times \mathrm{Re}[i^{l_0-l}g^*_{\lambda,m}(\theta)T^\Lambda_{vl,v_0l_0}] + \frac{\pi^2}{k_0^2}\sum_{l,l_0}^{l_B}\sum_{l',l_0'}^{l_B}\sum_{\Lambda,\Lambda'}\sum_L d_L(ll_0,l'l_0';\Lambda,\Lambda') \times T^{\Lambda*}_{vl,v_0,l_0}T^{\Lambda'}_{vl',v_0,l_0'}P_L(\cos\theta), \tag{16a}$$

where $d_L(ll_0,l'l_0';\Lambda,\Lambda')$ is defined in Eq. (6c) and $c_\lambda(lm,l_0m_0)$ in Eq. (14). The only previously undefined quantity in this equation is

$$g_{\lambda,m}(\theta) \equiv i^\lambda\left(\frac{8\pi}{2\lambda+1}\right)Y_{\lambda,m}(\hat{\boldsymbol{q}})\sum_\eta\langle v|b_{\lambda,\eta}|v_0\rangle M_\lambda^\eta(q_{v,v_0}) - \left(\frac{8\pi}{2\lambda+1}\right)\sum_{l,l_0}^{l_B} i^{l_0-l}Y_{lm}(\hat{\boldsymbol{k}})\sqrt{(2l_0+1)(2l+1)} \times c_\lambda(lm,l_00)\sum_\eta\langle v|b_{\lambda,\eta}|v_0\rangle M_{ll_0}^\eta(k_vk_0), \tag{16b}$$

The sum over L in Eq. (16a) runs from $L=0$ to $L=2l_B$, the maximum value allowed by the angular-momentum coupling coefficients in this expression. Since the lab-frame azimuthal angle ϕ is arbitrary for linear systems, we choose $\phi=0$, which implies that $\phi_q=\pi$ in Eq. (10b). With this choice all spherical harmonics in Eqs. (16a) and (16b) are real. For vibrationally elastic scattering, with $v=v_0$, and for long-range potentials for only $\lambda=0$ and $\lambda=2$, Eqs. (16a) and (16b) reduce to those of Isaacs and Morrison [10].

The physical content of the three terms in Eq. (16a) and (16b) is different. The first term involves only the long-range interaction and is purely Born in character. If one chooses $l_B=-1$, then the second and third terms vanish and one regains the pure Born approximation to the DCS. The third term involves no Born approximations; it is due solely to T-matrix elements for $l\le l_B$, which incorporate short- and intermediate-range interactions and make no weak-scattering approximations. If one sets l_B to ∞, then the sum of the first two terms vanishes and one regains the usual equation for the DCS in terms of BF-FNO T-matrix elements (see Ref. [2], and references therein). Finally, the second term introduces interference between non-Born T-matrix elements for $l<l_B$ and Born elements for $l\ge l_B$.

The practical advantage of the ABC strategy is that all sums over partial-wave order in the ABC DCS (16a) and (16b) terminate at l_B, the value of which is much smaller than the maximum values of l, l', l_0, and l_0' that would be required to numerically converge the DCS (6a)–(6c). This termination also limits the sums over the projection quantum number Λ. The sums over λ [in Eq. (16a)] and η [in Eq. (16b)] include only those terms chosen for the truncated multipole expansion (8b).

The integrals $I_\lambda^\eta(q_{v,v_0})$ and $I_{ll_0}^\eta(k_v k_0)$, which lead to the functions $M_\lambda^\eta(q_{v,v_0})$ and $M_{ll_0}^\eta(k_v k_0)$ in Eq. (16b), are defined in Eqs. (12b) and (13b). As we remarked in conjunction with the closed-form expressions (12c) and (13c), these integrals are formally undefined for one case that always arises in electron-molecule scattering. The spherically symmetric term in the long-range potential (8a), which contains the spherical polarizability $\alpha_0(R)$ and which corresponds to $\lambda=0$, $\eta=4$, and $b_{0,4}(R)=-\alpha_0(R)/2$, produces $I_0^4(q_{v,v_0})$ and $I_{00}^4(k_v k_0)$, neither of which is defined. But, in Eq. (16b) only the difference of the two integrals appears and this integral is defined. It evaluates to

$$\int_0^\infty [j_\lambda(q_{v,v_0}r) - j_l(k_v r) j_{l_0}(k_0 r)] r^{2-\eta} dr = -\pi\left(\frac{q_{v,v_0}}{4} + \frac{k_v^2 + 3k_0^2}{12k_0}\right) \tag{17}$$

which is the same result as that obtained from evaluating $M_0^4(q_{v,v_0}) - M_{00}^4(k_v k_0)$. This makes it possible to use the expressions for $M_\lambda^\eta(q_{v,v_0})$ and $M_{ll_0}^\eta(k_v k_0)$ in derivations without having to worry about the special cases mentioned in conjunction with Eqs. (12b) and (13b).

III. RESULTS

To illustrate the efficacy and accuracy of the ABC procedure, we have chosen two paradigmatic homonuclear systems: e-H_2 and e-N_2. No other systems have been so exhaustively studied both experimentally and theoretically (see, for example, Refs. [17,55–61], and references therein), and the high accuracy of cross sections for these systems has established them as benchmarks in the field. Calculating DCS for e-H_2 scattering should offer the fewest challenges, as H_2 is nearly spherical compared to other linear molecules. Moreover, only for e-H_2 do there exist converged BF-FNO, close-coupling T-matrix elements using a parameter-free interaction potential and including exchange effects exactly [56,62,63]. By contrast, the N_2 molecule is quite aspherical, and, as demonstrated in Ref. [17], a converged NBC calculation of low-energy e-N_2 DCS requires very many partial waves and symmetry classes. Moreover, e-N_2 scattering at energies between about 1.5 and 4.0 eV is dominated by an intermediate-duration shape resonance in the Π_g symmetry [17,41,64–68]. This resonance induces highly oscillatory behavior in differential and integral cross sections in this energy range and so offers a quite different physical context for calculating DCS.

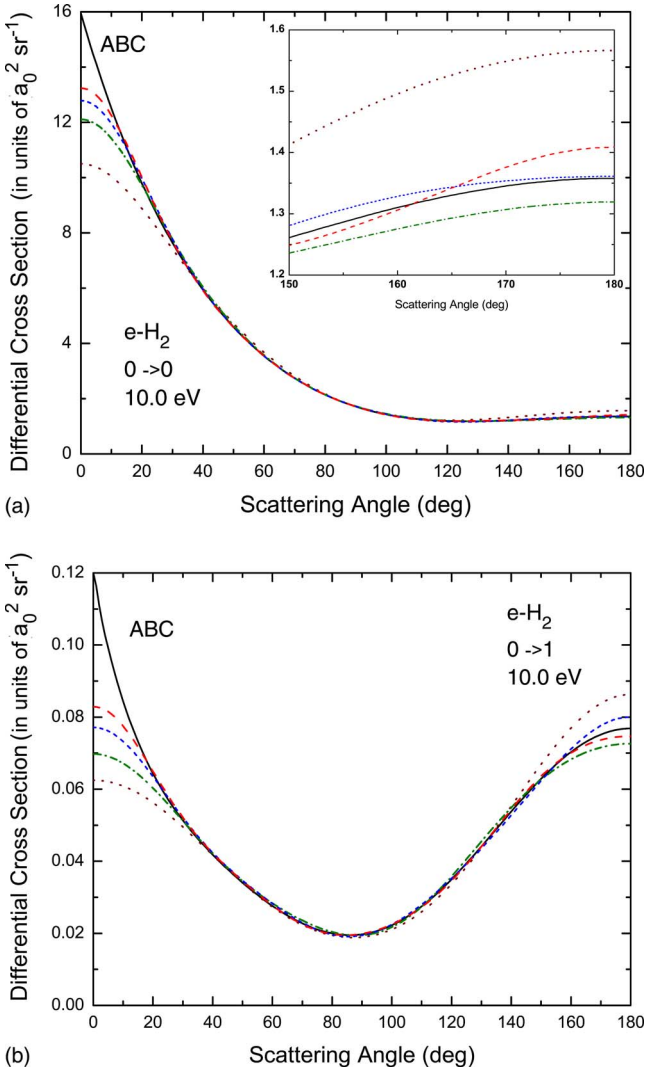

FIG. 1. (Color online) Convergence in partial-wave order and symmetry class of e-H_2 elastic (upper panel) and $0\rightarrow1$ inelastic (lower panel) DCS in numerical Born completion calculations at 10.0 eV. In each panel, the solid curve is the fully converged ABC DCS with $l_B=3$ (see Fig. 2), shown for comparison. The other curves correspond to increasing maximum values of $|\Lambda|$, the projection quantum number for the electron's orbital angular momentum in the exact DCS of Eqs. (6a)–(6c): $|\Lambda|=1$ (dotted), $|\Lambda|=2$ (dash-dot), $|\Lambda|=3$ (short dash), and $|\Lambda|=4$ (long dash). For each value of Λ_{max} we include partial-wave contributions in Eq. (6b) up to $l_{max}=\Lambda_{max}$. The inset figure in the upper panel expands the vertical scale for large-angle elastic scattering.

A. ABC DCS for e-H_2 scattering

To illustrate the need for high-order partial waves and to illuminate the angles at which they play the greatest role in a DCS we show in Fig. 1 elastic (upper panel) and inelastic $(v_0\rightarrow v)=(0\rightarrow1)$ (lower panel) DCS for e-H_2 collisions at 10.0 eV as calculated using numerical Born completion using Eqs. (6a)–(6c). (Equations for the FBA scattering matrix elements required for such a numerical treatment are given in Sec. III.A of Ref. [17] and the Appendix in Ref. [14].) As a benchmark for assessing convergence of these NBC cross

TABLE I. Vibrational matrix elements of permanent and induced moments for the e-H_2 and e-N_2 ABC DCS calculations in this paper. A description of computation of the e-N_2 moments appears in Sec. III.B of Ref. [17]; see also [32]; the R-dependent moments used in these computations come from structure calculations described in citations in these references. All matrix elements are in atomic units: a_0^3 for polarizabilities, ea_0^2 for the quadrupole moment.

		e-H_2		
v_0	v	$\langle v\|\alpha_0\|v_0\rangle$	$\langle v\|\alpha_2\|v_0\rangle$	$\langle v\|Q\|v_0\rangle$
0	0	5.3750	1.4119	0.4704
0	1	0.7970	0.4386	0.0903
0	2	−0.0467	0.0088	−0.0090
1	2	1.1853	0.6913	0.1399
		e-N_2		
v_0	v	$\langle v\|\alpha_0\|v_0\rangle$	$\langle v\|\alpha_2\|v_0\rangle$	$\langle v\|Q\|v_0\rangle$
0	0	10.980	3.0958	−0.9608
0	1	0.4075	0.3027	0.0881

sections we show the (fully converged) ABC cross sections, which include all T-matrix elements and are based on Eqs. (16a) and (16b).

In the long-range e-H_2 potential of Eq. (8a) we included permanent quadrupole and induced spherical and nonspherical polarizability terms; this choice determined the values of λ and η in these equations. Values of vibrational matrix elements of these moments for excitations considered in this section are given in Table I. At each energy we included Legendre polynomials of all required orders: $L=0$ to $L=2l_B$ in Eq. (16a); this integer controls the shape of the DCS, Eq. (1). Because these e-H_2 DCS vary weakly with angle, only the first few Legendre polynomials contribute appreciably. Finally, we computed the non-Born, BF-FNO e-H_2 T-matrix elements using the linear-algebraic method [69] including exact exchange, as described in Ref. [56].

Figure 1 illustrates the variation with scattering angle of the rate at which NBC DCS approach convergence. At small angles, by which we mean $\theta \lesssim 30°$ and, for elastic scattering at large angles $\theta \gtrsim 150°$ (shown in the inset), the approach to convergence is very gradual. The smaller the scattering angle, the more T-matrix elements must be included in the DCS. It may be surprising, considering the nearly spherical character of H_2, that inclusion even of matrix elements for $l \geq 4$, which correspond to the $|\Lambda|=4$ curve in the figures, fails to converge the small-angle DCS to graphical accuracy. In the far more aspherical e-N_2 system, partial waves of these and much higher orders are far more important (see Sec. III B).

To illustrate the need for only a few low-order non-Born T-matrix elements, we show in Fig. 2 inelastic $0 \rightarrow 1$ DCS for e-H_2 collisions at 1.0 and 10.0 eV. At each energy, we calculated ABC DCS for increasing values of l_B in Eqs. (16a) and (16b), the partial-wave order such that contributions from all T-matrix elements with $l > l_B$ are included via the FBA.

The presence in both plots in Fig. 2 of the pure-Born result, obtained by setting $l_B=-1$ in Eqs. (16a) and (16b), dramatically demonstrates the need for some non-Born contributions at these energies. At 1.0 eV, the most significant of these non-Born contributions for reshaping the DCS into something resembling the converged result are those for $l=0$, from the Σ_g symmetry class. At 10.0 eV, these $l=0$ matrix elements alone do not do the job. At both energies, however, including non-Born $l=1$ matrix elements (from Σ_g and Π_u symmetries) gives a qualitatively correct DCS; further including $l=2$ elements (from Σ_g and Π_g) gives DCS converged to experimental accuracy [56]; and including $l=3$ elements gives convergence to graphical accuracy. Consistent with the physical mechanism of centrifugal-barrier effects discussed in Sec. I, the importance of non-Born T-matrix elements with $l=3$ is larger at 10.0 eV than at 1.0 eV, a point that is obscured by the scale of the vertical axis in Fig. 2. The trends in these plots exemplify behavior we found at many other energies between threshold and 10.0 eV, not only for $0 \rightarrow 1$ excitations but also $0 \rightarrow 2$ and $1 \rightarrow 2$ (not shown). For e-H_2 scattering and for nonresonant scattering in e-N_2 (Sec. III B), we find the choice of l_B that guarantees a particular precision in a particular DCS to be quite insensitive to scattering energy and excitation.

In choosing l_B, it is essential to appreciate that, because T-matrix elements of different symmetry classes and partial-wave orders commingle in the DCS (6a)–(6c), not all such elements must be calculated to the same precision. Choosing l_B by direct comparison of non-Born and Born-T-matrix elements would be overkill.

Nevertheless, the concerns of this paper raise the question of how accurately the FBA does approximate key T-matrix elements of fairly low order. Examining individual matrix elements for e-H_2 (not shown) we find several trends. First, as partial-wave order increases, the FBA becomes more accurate. Second, as energy increases for a particular excitation and partial-wave order, the FBA becomes less accurate, owing to increased penetration of the corresponding components of the radial scattering function into the strong near- and intermediate-target regions [1,22,42]. Consequently, inclusion of even fairly inaccurate FBA T-matrix elements in exact ABC-DCS calculations [Eqs. (6a)–(6c), (16a), and (16b)] does not contaminate the cross sections themselves.

B. ABC DCS for e-N_2 scattering

For converging DCS, the most important difference between the e-H_2 and e-N_2 systems is the greater strength of the short- and intermediate-range e-N_2 potential; this difference is largely a consequence of the stronger nuclear attraction in e-N_2. For given quantum numbers $(l,l';\Lambda)$ of reasonably small order, therefore, one would expect the error in the FBA e-N_2 T-matrix element, compared to its BF-FNO counterpart, to be greater than for e-H_2. Moreover, one would expect to need more T matrix elements in a brute-force numerical completion calculation using Eqs. (6a)–(6c). One would be right. Examination of individual T-matrix elements shows the FBA to be far less accurate for N_2 than for H_2. Moreover, for high-order partial waves, this inaccuracy is more severe for N_2 than for H_2. For sufficiently large values of l, however, we find good agreement between the FBA and BF-FNO elements.

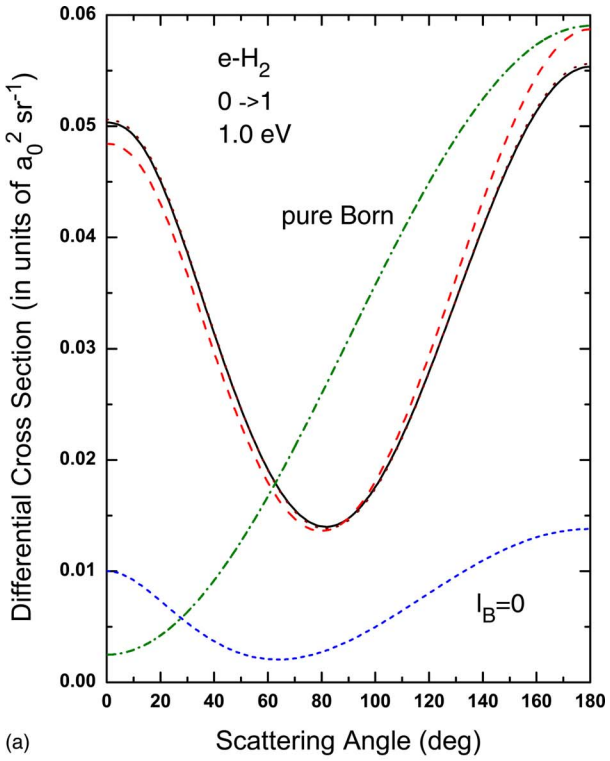

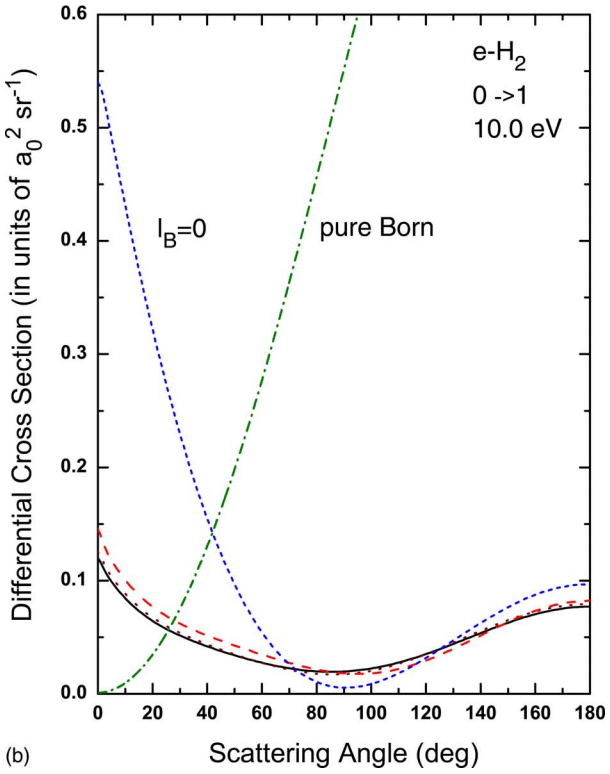

FIG. 2. (Color online) The contribution of non-Born elements of the BF-FNO T matrix to e-H_2 DCS at 1.0 eV (upper panel) and 10.0 eV (lower panel). The dot-dashed curves are pure FBA ($l_B=-1$); the 10.0 eV pure-FBA $0\rightarrow1$ DCS in the lower panel goes off scale to a maximum value at 180° in units of 1.1 a_0^2. The other curves correspond to increasing values of l_B: $l_B=0$ (short dash), $l_B=1$ (long dash), $l_B=2$ (dotted), and $l_B=3$ (solid). At both energies, the $l_B=2$ and $l_B=3$ curves are indistinguishable, indicating convergence in l_B.

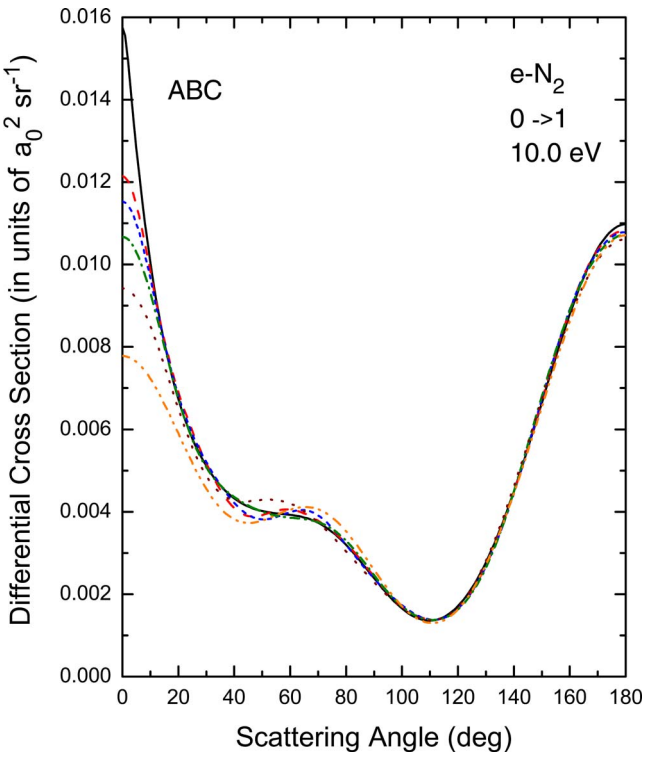

FIG. 3. (Color online) Convergence in partial-wave order and symmetry class of e-N_2 DCS for $0\rightarrow1$ vibrational excitation in numerical Born completion calculations at 10.0 eV. The solid curve is the fully converged ABC DCS with $l_B=5$. The other curves correspond to increasing maximum values $|\Lambda|=2$ (dotted), $|\Lambda|=4$ (dash-dot), $|\Lambda|=6$ (short dash), $|\Lambda|=8$ (long dash), and $|\Lambda|=10$ (dash-dot-dot).

As remarked above, this decrease in accuracy of FBA T-matrix elements in the transition from H_2 to N_2 results from the far stronger e-N_2 short-range interaction potential. But interpreting the comparison between e-H_2 and e-N_2 DCS is not quite this simple. The long-range interaction potential for e-N_2 is appreciably stronger than for e-H_2, a dissimilarity evident in the moments in Table I. To clarify the role of partial waves in this system, therefore, we must also examine directly convergence of DCS.

In a detailed study of numerical Born completion for elastic and inelastic e-N_2 scattering Sun *et al.* [17] demonstrated (see their Sec. III.C) that in the resonance-dominated region from about 1.5 to about 4.0 eV, T-matrix elements for high-order partial waves and symmetry classes make negligible contribution to the DCS. This insensitivity arises from the approximate localization of the scattering electron's probability density near the target in near-resonant scattering [44].

Nonresonant scattering is another story. Outside the resonance region, Sun *et al.* found T-matrix elements for $|\Lambda|\leq7$ to be essential for converging elastic and inelastic DCS, especially at scattering angles $\theta\lesssim60°$ (see their Fig. 3). For $\theta\leq45°$, Sun *et al.* required T-matrix elements for $|\Lambda|\leq8$ (17 symmetry classes) to converge inelastic DCS. For other excitations, T matrices from as many as 25 symmetry classes were required before the effort to converge the DCS numerically via Born completion was abandoned because of

numerical problems attendant upon implementing the FBA for such high-order partial waves. All these problems, as well as the odious chore of determining the maximum required value of $|\Lambda|$, vanish when one uses analytic rather than numerical Born completion.

In Figs. 3 and 4 we show $0\rightarrow1$ DCS for collisions with N_2 at 10.0 eV. The shape of this DCS is more complicated than its counterpart for e-H_2 scattering in Fig. 1, primarily because of greater influence on BF-FNO T matrix elements of short- and intermediate-range interactions.

Figure 4 shows the $0\rightarrow1$ cross section for increasing values of l_B from e-N_2 ABC calculations at two energies chosen to illustrate near-resonant and nonresonant scattering. At 5.0 eV, above but within the influence of the 2.39 eV shape resonance, scattering in the $^2\Pi_g$ resonant symmetry still dominates the DCS. On the one hand, one must treat the resonant $l=2$ partial wave accurately, not by the FBA; on the other, having done so, one need not include higher-order partial waves at all.

With increasing energy, the resonance loses potency. By 10.0 eV, converging the nonresonant DCS in Fig. 4 requires far more partial waves than did the near-resonant DCS. Inclusion of BF-FNO T-matrix elements for only $l=0$ and 1 produces a DCS whose shape is only roughly correct, in contrast to the corresponding e-H_2 case in Fig. 2. Another difference between these two systems is the somewhat slower convergence with increasing l_B for e-N_2 than for e-H_2. This difference, similar to the one discussed in conjunction with Fig. 3, is due primarily to the greater strength of the short- and intermediate-range e-N_2 potential.

For nonresonant e-N_2 scattering we found the brute-force numerical completion procedure to be impractical. Figure 3 shows that, as for e-H_2 (Fig. 1), increasing the maximum value of Λ in a numerical e-N_2 Born-completion calculation does eventually converge the DCS expansion (6a)–(6c). But for e-N_2, convergence is much slower than for e-H_2, except at large angles. At small angles, even an NBC cross section for $\Lambda_{max}=10$ (21 symmetries) is incorrect in magnitude at small angles and in shape at intermediate angles.

Higher-order partial waves do contribute to the corresponding integral cross section

$$\sigma_{0\rightarrow1}(E) \equiv \int_{4\pi} \frac{d\sigma}{d\Omega}(\boldsymbol{k}_v,\boldsymbol{k}_0)d\Omega, \tag{18a}$$

and to the momentum-transfer cross section

$$\sigma^{(m)}_{0\rightarrow1}(E) \equiv \int_{4\pi} \frac{d\sigma}{d\Omega}(\boldsymbol{k}_v,\boldsymbol{k}_0)(1-\cos\,\theta)d\Omega. \tag{18b}$$

The contribution of high-order partial waves to these integrated cross sections is far less striking than to DCS. Still, these contributions are material in applications that require high-precision integrated cross sections. Table II shows convergence of integrated $0\rightarrow1$ cross sections for the e-N_2 convergence studies whose DCS appear in Figs. 3 and 4.

IV. CONCLUSION

The key theoretical result of this research is Eqs. (16a) and (16b) for the vibrationally inelastic DCS in the ABC

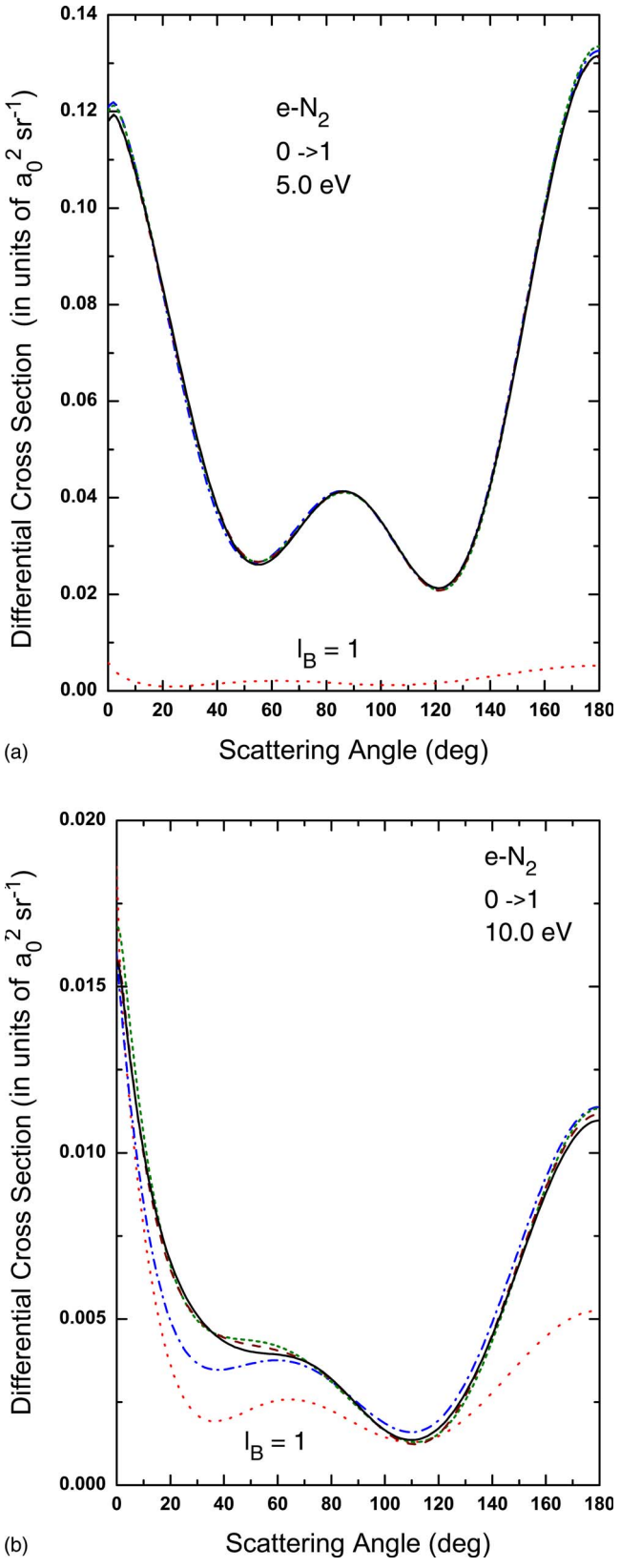

FIG. 4. (Color online) The contribution of non-Born elements of the BF-FNO T matrix to e-N_2 DCS at 5.0 eV (upper panel) and 10.0 eV (lower panel). In each graph, each curve corresponds to a larger value of l_B, as $l_B=1$ (dotted), $l_B=2$ (dot-dash), $l_B=3$ (short dash), $l_B=4$ (long dash), and $l_B=5$ (solid).

TABLE II. Integrated e-N_2 cross sections ($10^2 \times a_0^2$) at 10.0 eV from two convergence studies. The top table, which corresponds to DCS in Fig. 4, shows integral cross sections $\sigma_{0\to1}$ and momentum-transfer cross sections $\sigma_{0\to1}^{(m)}$ for increasing values of l_B in Eqs. (16a) and (16b). The bottom table, which corresponds to the DCS in Fig. 3, shows cross sections for increasing maximum values of Λ in numerical Born completion calculations performed using Eq. (6a)–(6c).

Convergence with respect to l_B in ABC calculations		
l_B	$\sigma_{0\to1}$	$\sigma_{0\to1}^{(m)}$
1	2.9660	2.92130
2	4.5769	4.79570
3	4.7113	4.52414
4	4.6976	4.55633
5	4.6989	4.56626
Convergence with respect to $\Lambda_{\max}$ in NBC calculations		
$\Lambda_{\max}$	$\sigma_{0\to1}$	$\sigma_{0\to1}^{(m)}$
2	4.58611	4.56480
4	4.66206	4.57007
6	4.68614	4.57547
8	4.69344	4.57380
10	4.69688	4.57320

method, together with the attendant definitions of quantities in this expression. Users will need the functions $M_\lambda^\eta(q_{v,v_0})$ and $M_{ll_0}^\eta(k_v k_0)$ [Eqs. (12c) and (13c)]. These equations can be easily encoded, and upon request the authors will supply either MATHEMATICA notebooks or FORTRAN subroutines that evaluate them.

The e-H_2 and e-N_2 calculations reported in Sec. III demonstrate two key points. First, the ABC procedure is an extremely efficient way to guarantee convergence of DCS compared to numerical Born completion, which, if feasible at all, requires convergence studies that are obviated by the ABC approach. Second, the number of non-Born T-matrix elements required to determine a DCS to a desired accurate is quite small—smaller than one might expect from a direct comparison of T-matrix elements.

As illustrated in previous research discussed in Sec. I, the underlying idea of analytic Born completion is not limited to the linear molecules considered here. Neither are the equations of Sec. II D limited to homonuclear targets. For heteronuclear targets, however, implementation of the ABC equations requires that one deal with a well-known technical problem that afflicts electron scattering from polar molecules: the singularity in the body-frame DCS in the zero-angle limit [70]. This defect, which inheres in the FNO approximation and has nothing to do with use of the FBA, can be repaired in various ways [6–8,11,60,71–74].

As contributions to the economics of electron scattering calculations, analytic Born completion procedures offer two practical advantages: they eliminate the need to calculate individual high-order T-matrix elements and to operationally converge the DCS with respect to partial waves. Calculating T-matrix elements of high order in, say, a BF-FNO calculation is certainly inadvisable: these elements are small so their calculation is prone to numerical error. Computing high-order T-matrix elements in the FBA for a numerical Born completion calculation is more efficient but requires converging several sums over partial-wave order and electron-molecule symmetry classes [see Eqs. (6a)–(6c)]. As illustrated for both e-H_2 and e-N_2 in Sec. III, brute-force numerical convergence—especially at angles less than about 30°—may be quite hard or even impossible to achieve in practice.

ACKNOWLEDGMENTS

The authors are grateful to Dr. Bill Isaacs and Mr. Olen Boydstun for contributions to early stages of this research and to Professor Itikawa for drawing our attention to an error in our original implementation of ABC to vibrationally elastic scattering. Special thanks go to Drs. Tom Rescigno and Bill McCurdy for providing T-matrix elements for some of our test cases and to Drs. R. P. McEachran and Ilya Fabrikant for useful discussions on various aspects of this research. This project was supported in part by the National Science Foundation under Grant No. PHY-0354858.

[1] N. F. Lane, Rev. Mod. Phys. **52**, 29 (1980).
[2] M. A. Morrison and W. Sun, in *Computational Methods for Electron-Molecule Collisions*, edited by W. Huo and F. Gianturco (Plenum, New York, 1995), Chap. 6, pp. 131–190.
[3] D. G. Thompson, Proc. R. Soc. London, Ser. A **294**, 160 (1966).
[4] O. H. Crawford and A. Dalgarno, J. Phys. B **4**, 494 (1971).
[5] A. W. Fliflet and V. McKoy, Phys. Rev. A **21**, 1863 (1980).
[6] D. W. Norcross and N. T. Padial, Phys. Rev. A **25**, 226 (1982).
[7] T. N. Rescigno and B. I. Schneider, Phys. Rev. A **45**, 2894 (1992).
[8] T. N. Rescigno, B. H. Lengsfield, C. W. McCurdy, and S. D. Parker, Phys. Rev. A **45**, 7800 (1992).
[9] W. A. Isaacs and M. A. Morrison, Phys. Rev. A **53**, 4215 (1996).
[10] W. A. Isaacs and M. A. Morrison, Phys. Rev. A **54**, 3697 (1996).
[11] Y. Itikawa, Theor. Chem. Acc. **105**, 123 (2000).
[12] I. Fabrikant, Sov. Phys. JETP **44**, 77 (1976).
[13] N. Chandra, Phys. Rev. A **16**, 80 (1977).
[14] M. A. Morrison, A. N. Feldt, and D. Austin, Phys. Rev. A **29**, 2518 (1984).
[15] T. L. Gibson, M. A. P. Lima, V. McKoy, and W. M. Huo, Phys. Rev. A **35**, 2473 (1987).
[16] H. T. Thümmel, R. K. Nesbet, and S. D. Peyerimhoff, J. Phys. B **25**, 4553 (1992).

[17] W. Sun, M. A. Morrison, W. A. Isaacs, W. K. Trail, D. T. Alle, R. J. Gulley, M. J. Brennan, and S. J. Buckman, Phys. Rev. A **52**, 1229 (1995).

[18] In principle, of course, one could generate all required T-matrix elements directly from BF-FNO calculations; this approach, which procedure one could characterize as circumvented non-Born cross sections (CBS) generation, is impractical and will not be pursued here.

[19] C. T. Whelan and B. Piraux, Phys. Lett. A **122**, 126 (1987).

[20] J. M. Wadehra and S. N. Nahar, Phys. Rev. A **36**, 1458 (1987).

[21] I. Linert, B. Mielewska, G. C. King, and M. Zubek, Phys. Rev. A **74**, 042701 (2006).

[22] M. A. Morrison, Adv. At. Mol. Phys. **24**, 51 (1988).

[23] U. Fano and D. Dill, Phys. Rev. A **6**, 185 (1972).

[24] B. I. Schneider and T. N. Rescigno, Phys. Rev. A **37**, 3749 (1988).

[25] D. A. Przybyla, W. Addo-Asah, W. E. Kauppila, C. K. Kwan, and T. S. Stein, Phys. Rev. A **60**, 359 (1999).

[26] M. Takekawa and Y. Itikawa, J. Phys. B **32**, 4209 (1999).

[27] M. Shimoi and Y. Itikawa, J. Phys. B **32**, 65 (1999).

[28] A. P. P. Natalense, M. T. do N. Varella, M. H. F. Bettega, L. G. Ferreira, and M. A. P. Lima, J. Phys. B **32**, 5523 (1999).

[29] M. Ingr, M. Polášek, P. Carsky, and J. Horáček, Phys. Rev. A **62**, 032703 (2000).

[30] R. K. Nesbet, S. Mazevet, and M. A. Morrison, Phys. Rev. A **64**, 034702 (2001).

[31] F. A. Gianturco and T. Stoecklin, J. Phys. B **34**, 1695 (2001).

[32] H. Feng, W. Sun, and M. A. Morrison, Phys. Rev. A **68**, 062709 (2003).

[33] L. U. Ancarani and M. C. Chidichimo, J. Phys. B **37**, 4339 (2004).

[34] T. N. Rescigno, W. A. Isaacs, A. E. Orel, H. D. Meyer, and C. W. McCrudy, Phys. Rev. A **65**, 032716 (2002).

[35] In electron scattering the "body-frame" is a reference frame in which the set of operators that defines the basis for expansion of the electron-molecule wave function includes the projection along the internuclear axis of the electronic orbital angular momentum of the system, which for a closed-shell target equals that of the scattering electron [1,42]. In the FNO approximation, the commutator of the rotational Hamiltonian and the interaction potential is dropped from the scattering equations. This step aligns the polar axis of the body frame with the internuclear axis and, in effect, "freezes" the target orientation for the duration of the collision (see Ref. [22], and references therein). Unless rotational excitation cross sections are required, one allows for the rotational dynamics "after the fact" by averaging over internuclear orientations [36,37,40].

[36] D. M. Chase, Phys. Rev. **104**, 838 (1956).

[37] A. Temkin and K. V. Vasavada, Phys. Rev. **160**, 109 (1967).

[38] A. N. Feldt and M. A. Morrison, J. Phys. B **15**, 301 (1982).

[39] M. A. Morrison, A. N. Feldt, and B. C. Saha, Phys. Rev. A **30**, 2811 (1984).

[40] N. Chandra and A. Temkin, Phys. Rev. A **13**, 188 (1976).

[41] C. A. Weatherford and A. Temkin, Phys. Rev. A **49**, 2580 (1994).

[42] M. A. Morrison, Aust. J. Phys. **36**, 239 (1983).

[43] Throughout this paper we use the "default" conventions for normalizing continuum functions and relating the S and T matrices, as described in Morrison and Feldt [45]. To change conventions, one need only multiply the T matrices by β/ζ^2, where β and ζ are defined in Ref. [45], before inserting these matrix elements in the equations presented here.

[44] J. R. Taylor, *Scattering Theory* (Wiley, New York, NY, 1972).

[45] M. A. Morrison and A. N. Feldt, Am. J. Phys. **75**, 67 (2007).

[46] F. A. Gianturco, R. R. Lucchese, N. Sanna, and A. Talamo, in *Electron Collisions with Molecules, Clusters, and Surfaces*, edited by H. Ehrhardt and L. A. Morgan (Plenum Press, New York, 1994), pp. 71–86.

[47] D. M. Brink and G. R. Satchler, *Angular Momentum*, 3rd ed. (Clarendon Press, Oxford, 1993).

[48] D. A. Varshalovich, A. N. Moskalev, and V. K. Khersonskii, *Quantum Theory of Angular Momentum* (World Scientific, New Jersey, 1988).

[49] Each value of $|\Lambda|$ and, for homonuclear molecules, the parity of the nuclear geometry (gerade or ungerade) defines an electron-molecule symmetry class. The BF-FNO T matrix is block diagonal with respect to this symmetry class. A given value of Λ and the parity determine the minimum value of l in the corresponding block: for $\Lambda=0$, the $^1\Sigma_g$ T matrix contains T^{Λ}_{vl,v_0l_0} for even $l\geq 0$, while the $^1\Sigma_u$ T matrix contains elements for odd $l\geq 1$. For further discussion see Refs. [1,22,42].

[50] Various definitions of the permanent quadrupole moment in the long-range interaction potential appear in the literature. We define this quantity (in atomic units) as (Ref. [51], Sec. 2.1.2) $Q(R)\equiv(1/2)\int\rho(\boldsymbol{r},R)(3xy-r^2)d\boldsymbol{r}^3$, where $\rho(\boldsymbol{r},R)$ is the one-electron density function of the target at internuclear separation R.

[51] I. G. Kaplan, *Interrmolecular Iteractions: Physical Pictures, Computational Methods, and Model Potentials* (Wiley, New York, 2006).

[52] M. A. Morrison, N. F. Lane, and L. A. Collins, Phys. Rev. A **15**, 2186 (1977).

[53] G. B. Arfken and H. J. Weber, *Mathematical Methods for Physicists*, 6th ed. (Elsevier, New York, 2005).

[54] M. E. Rose, *Elementary Theory of Angular Momentum* (Wiley, New York, 1957).

[55] R. W. Crompton and M. A. Morrison, in *Swarm Studies and Inelastic Electron-Molecule Collisions*, edited by L. C. Pitchford, V. McKoy, A. Chutjian, and S. Trajmar (Springer, New York, 1987), p. 43.

[56] S. J. Buckman, M. J. Brunger, D. S. Newman, G. Snitchler, S. Alston, D. W. Norcross, M. A. Morrison, B. C. Saha, G. Danby, and W. K. Trail, Phys. Rev. Lett. **65**, 3253 (1990).

[57] A. G. Robertson, M. T. Elford, R. W. Crompton, M. A. Morrison, W. Sun, and W. K. Trail, Aust. J. Phys. **50**, 441 (1997).

[58] M. T. Elford, R. W. Crompton, M. J. Brennan, M. A. Morrison, W. A. Isaacs, W. Sun, and W. K. Trail, Aust. J. Phys. **50**, 441 (1997).

[59] M. Allan, J. Phys. B **38**, 3655 (2005).

[60] Y. Itikawa and N. Mason, Phys. Rep. **414**, 1 (2005).

[61] J. Horáček, M. Čížek, K. Houfek, P. Kolorenč, and W. Domcke, Phys. Rev. A **73**, 022701 (2006).

[62] W. K. Trail, Ph.D. thesis, University of Oklahoma, Norman, Oklahoma (1991).

[63] M. A. Morrison and W. K. Trail, Phys. Rev. A **48**, 2874 (1993).

[64] J. N. Bardsley and F. Mandl, Rep. Prog. Phys. **31**, 471 (1968).

[65] L. Dubé and A. Herzenberg, Phys. Rev. A **20**, 194 (1979).

[66] T. N. Rescigno, A. E. Orel, and C. W. McCurdy, J. Chem. Phys. **73**, 6347 (1980).

[67] A. U. Hazi, T. N. Rescigno, and M. Kurilla, Phys. Rev. A **23**, 1089 (1981).
[68] P. L. Gertitschke and W. Domcke, J. Phys. B **26**, 2927 (1993).
[69] B. I. Schneider and L. A. Collins, Comput. Phys. Rep. **10**, 49 (1989).
[70] D. W. Norcross and L. A. Collins, Adv. At. Mol. Phys. **18**, 341 (1982).
[71] Y. Itikawa, Phys. Essays **13**, 344 (2000).
[72] The focus of Itikawa's development [11], similar to that of its precursor, the MEAN approximation of Norcross and Padial [6], is scattering from a polar molecule, although Itikawa [11] also gives useful equations for purely quadrupole and/or induced-dipole interactions for elastic scattering. He also gives a form for inelastic scattering from a dipole potential, but stops short of giving the full equations for a completely analytic form that applies to any long-range potential. Our formulation applies to any combination of long-range potentials, including dipole, though we only show the utility when applied to homonuclear systems. Itikawa transforms the BF scattering amplitude into the lab frame with channels identified by rotational as well as vibrational quantum numbers. Averaging and summing over initial and final rotational sublevels, respectively, in the adiabatic-nuclear-rotation approximation [73] is followed by introduction of the Born approximation for the scattering amplitude using the long-range potential Eq. (8a), as we do in Sec. II. To obtain cross sections for vibrational excitation, Itikawa sums over all final-state rotational quantum number; in the adiabatic-nuclear-rotation approximation this sum does not depend on the initial rotational-state quantum number (Refs. [1,14,22], and references therein). Previously Shimoi and Itikawa [27] applied this approach to rotational excitation of HCl (in the rigid-rotor approximation) as did Takekawa and Itikawa [74] to dipole-allowed excitations of CO_2. None of these papers address the issues of convergence or accuracy we consider in Sec. III.
[73] E. S. Chang and A. Temkin, J. Phys. Soc. Jpn. **29**, 172 (1960).
[74] M. Takekawa and Y. Itikawa, J. Phys. B **31**, 3245 (1998).